Antioxidants and Redox Signaling

DOI: 10.1089/ars.2018.7718

Original Research Communication

Mutations in *RHOT1* disrupt ER-mitochondria contact sites interfering with calcium homeostasis and mitochondrial dynamics in Parkinson's disease

Dajana Grossmann[1] PhD, Clara Berenguer-Escuder[1] MSc, Marie Estelle Bellet[1] BSc, David Scheibner[2], Jill Bohler[1] MSc, Francois Massart[1] BSc, Doron Rapaport[3] PhD, Alexander Skupin[1, 4] PhD, Aymeric Fouquier d'Hérouël[1] PhD, Manu Sharma[5] PhD, Jenny Ghelfi[1] BSc, Aleksandar Rakovic[7] PhD, Peter Lichtner[6] PhD, Paul Antony[1] PhD, Enrico Glaab[1] PhD, Patrick May[1] PhD, Kai Stefan Dimmer[3] PhD, Julia Catherine Fitzgerald[2] PhD, Anne Grünewald*[1, 7] PhD, Rejko Krüger*[1, 2, 8] MD

* These authors share senior authorship.

1) Luxembourg Centre for Systems Biomedicine (LCSB), University of Luxembourg, Esch-sur-Alzette, Luxembourg

2) Department of Neurodegenerative Diseases, Center of Neurology and Hertie-Institute for Clinical Brain Research, University of Tübingen, Tübingen, Germany

3) Interfaculty Institute of Biochemistry (IFIB), University of Tübingen, Tübingen, Germany

4) National Biomedical Computation Resource, University California San Diego, La Jolla, CA, USA.

5) Centre for Genetic Epidemiology, Institute for Clinical Epidemiology and Applied Biometry, University of Tübingen, Tübingen, Germany

6) Institute of Human Genetics, Helmholtz Zentrum München GmbH, Neuherberg, Germany

7) Institute of Neurogenetics, University of Lübeck, Lübeck, Germany

8) Parkinson Research Clinic, Centre Hospitalier de Luxembourg (CHL), Luxembourg, Luxembourg

Running title: ***RHOT1* mutations disrupt ER-mitochondria contacts**

Corresponding authors: Dajana Grossmann (dajana.grossmann@uni.lu)

Rejko Krüger (rejko.krueger@uni.lu)

University of Luxembourg

Luxembourg Centre for Systems Biomedicine (LCSB)

7, avenue des Hauts-Fourneaux

L-4362 Esch-sur-Alzette

Luxembourg

Telephone: (+352) 46 66 44 5911

Fax: (+352) 46 66 44 35907

characters title: 127

words manuscript: 4913

reference numbers: 53

number figures grey: 0

number figures colour: 7

Antioxidants and Redox Signaling

Mutations in *RHOT1* disrupt ER-mitochondria contact sites interfering with calcium homeostasis and mitochondrial dynamics in Parkinson's disease (DOI: 10.1089/ars.2018.7718)

This paper has been peer-reviewed and accepted for publication, but has yet to undergo copyediting and proof correction. The final published version may differ from this proof.

Abstract

Objective: The outer mitochondrial membrane protein Miro1 is a crucial player in mitochondrial dynamics and calcium homeostasis. Recent evidence indicated that Miro1 mediates calcium-induced mitochondrial shape transition (MiST), which is a prerequisite for the initiation of mitophagy. Moreover, altered Miro1 protein levels have emerged as a shared feature of monogenic and sporadic Parkinson's disease (PD), but, so far, no disease-associated variants in *RHOT1* have been identified. **Results**: Here, for the first time, we describe heterozygous *RHOT1* mutations in two PD patients (het c.815G>A; het c.1348C>T) and identified mitochondrial phenotypes with reduced mitochondrial mass in patient-derived cellular models. Both mutations lead to decreased ER-mitochondrial contact sites and calcium dyshomeostasis. As a consequence, energy metabolism was impaired, which in turn lead to increased mitophagy. **Conclusion**: In summary, our data support the role of Miro1 in maintaining calcium homeostasis and mitochondrial quality control in PD.

Antioxidants and Redox Signaling
Mutations in *RHOT1* disrupt ER-mitochondria contact sites interfering with calcium homeostasis and mitochondrial dynamics in Parkinson's disease (DOI: 10.1089/ars.2018.7718)
This paper has been peer-reviewed and accepted for publication, but has yet to undergo copyediting and proof correction. The final published version may differ from this proof.

Antioxidants and Redox Signaling
Mutations in *RHOT1* disrupt ER-mitochondria contact sites interfering with calcium homeostasis and mitochondrial dynamics in Parkinson's disease (DOI: 10.1089/ars.2018.7718)
This paper has been peer-reviewed and accepted for publication, but has yet to undergo copyediting and proof correction. The final published version may differ from this proof.

Introduction

The mitochondrial Rho GTPase Miro1 has primarily been studied with respect to its function as an adaptor protein for mitochondrial transport [1][2], yet far less is known about the involvement of Miro1 in other processes crucial for maintaining mitochondrial homeostasis, such as mitochondrial calcium handling [3], mitochondrial quality control [2][4] and overall mitochondrial homeostasis [5]. Miro1 contains an N-terminal GTPase domain, followed by two calcium-binding EF-hand domains, a second C-terminal GTPase domain and the C-terminal transmembrane domain. The GTPase domains are involved in the control of mitochondrial movement [6] and in the regulation of mitochondrial calcium uptake [7] via the mitochondrial calcium uniporter (MCU) [3]. The calcium binding motifs of Miro1 are suggested to ensure the proper spatial arrangement of mitochondrial networks [1][8][9] as well as mitochondrial calcium uptake [3].

An initial link between Miro1 and PD arose from the identification of Miro1 as a target of the PD-associated kinase PINK1 (PARK6) in a mitochondrial quality control pathway [4]. Mitochondrial arrest is an important initial step required to isolate dysfunctional mitochondria and to prevent their fusion with healthy mitochondria. As a consequence, immobile fragmented mitochondria are primed for autophagosomal uptake and lysosomal degradation [4]. Moreover, in monogenic and sporadic PD an impairment of Miro1 degradation and mitochondrial dynamics was identified as a central component in neurodegeneration [10].

A recent study in embryonic fibroblasts from Miro1-mutant mice provided evidence for a link between the calcium-sensing function of Miro1 and mitochondrial shape transition (MiST), which is a crucial pre-requisite for subsequent mitophagy [9].

Here, we report the identification of mutations in *RHOT1*, the gene encoding Miro1, in PD patients and describe their pathogenic role in the maintenance of ER-mitochondria contact sites, cellular calcium homeostasis, and energy metabolism. Our phenotypic characterization in patient-derived cells points at the multifaceted roles of Miro1 at the outer mitochondrial membrane and highlights the significance of the protein for calcium homeostasis and mitochondrial impairment related to the pathogenesis of PD.

Results

Identification of R272Q and R450C RHOT1 variants in PD patients

Since several studies suggested that variants in *RHOT1* may confer risk to develop PD [2][11][12], we performed a comprehensive genetic screening for mutations in *RHOT1* in PD patients. In a German cohort of 752 PD patients and a total of 374 healthy controls, we identified two female patients carrying a heterozygous mutation c.815G>A or c.1348C>T in *RHOT1* (NM_001033568), leading to the amino acid exchanges R272Q and R450C, respectively (**Figure 1A**). The amino acid R272 is positioned within the ligand mimic motif of the first EF-hand domain [13] and the residue R450 lies within the C-terminal GTPase domain (**Figure 1A**). According to the homology model of the human Miro1 protein, the affected amino acids are exposed to the cytosol on the protein surface (**Figure 1C**). Different *in silico* prediction methods revealed a high likelihood for both mutations to have pathogenic effects (**Figure 1D**). Medical records of the fathers of both index patients revealed an unclassified tremor (**Figure 1B**). Due to the typical late onset and family history for motor symptoms, both patients were also tested for GBA and LRRK2 mutations. This analysis excluded the GBA N370S and L444P, and the LRRK2 G2019S and I2020T mutations by Sanger sequencing in both patients.

To identify additional carriers of the herein described *RHOT1* variants, we next searched a whole exome database on neurodegenerative diseases containing 1500 patient genomes. This approach revealed no additional carrier of R272Q or R450C mutations. Additional genotyping of 1238 German PD patients [14] and 662 healthy controls (KORA cohort) provided no further carriers of the R272Q or R450C mutation (**Figure 1E**).

Using the gnomAD browser to assess the genetic burden of *RHOT1* mutations in the general population, we found a lower amount of missense mutations than expected (missense z-score = 2.47) and a constraint for loss-of-function mutations (o/e score = 0.2; pLI score = 0.8; **Figure 1F**), which further supports a potential pathogenic role of damaging mutations in *RHOT1*.

In the gnomAD database, we found no additional carrier of the R272Q variant, but three carriers of the R450C variant (allele frequency 1.06e-5; https://gnomad.broadinstitute.org/variant/17-30530924-C-T?dataset=gnomad_r2_1). Two of these individuals are of European ancestry and the third individual of East Asian origin.

Antioxidants and Redox Signaling
Mutations in *RHOT1* disrupt ER-mitochondria contact sites interfering with calcium homeostasis and mitochondrial dynamics in Parkinson's disease (DOI: 10.1089/ars.2018.7718)
This paper has been peer-reviewed and accepted for publication, but has yet to undergo copyediting and proof correction. The final published version may differ from this proof.

All carriers of the R450C variant are heterozygous and their age was between 30 and 35 years. As our patients carrying Miro1 mutations presented with typical late-onset PD, it cannot be excluded that these individuals will develop PD later in life.

From these results we conclude that damaging mutations in *RHOT1* are a rare event, and suggest that mutations may contribute to the development of PD.

Reduced calcium buffering capacity in Miro1-mutant fibroblasts

One important function of Miro1 is the maintenance of mitochondrial calcium homeostasis [3][7], which is regulated by the calcium-binding EF-hand motifs and the C-terminal GTPase domain [7]. In order to assess effects of mutant Miro1 on calcium homeostasis, we used the cytosolic calcium indicator Fluo4-AM. Cells were treated with thapsigargin (an inhibitor of the SERCA pumps [15]), which prevents calcium buffering by the endoplasmic reticulum (ER) (**Figure 2A**) and causes an increase of cytosolic calcium by depletion of ER calcium stores [16]. In control cells, cytosolic calcium levels decreased within 5 min, whereas in Miro1-R272Q and in Miro1-R450C fibroblasts the cytosolic calcium content remained increased (**Figure 2B, C**). The alteration of calcium handling was also reflected by significantly increased time constants of exponential decay, calculated from the calcium response curves after treatment with thapsigargin (**Figure 2C**), in both Miro1-mutant fibroblast lines compared to controls (**Figure 2D**). To distinguish whether the altered calcium profiles in mutant fibroblasts were due to impaired mitochondrial calcium buffering or a reduced calcium release across the plasma membrane, we next treated the cells with Ru360, an inhibitor of the MCU [3][17][18], alone, or in combination with thapsigargin (**Figure 2E, G**). Blocking of the MCU after thapsigargin treatment led to a reduced buffering capacity of cytosolic calcium in mutant and control cells (**Figure 2E**). This observation was confirmed by calculation of the linear regression of the calcium response to concomitant thapsigargin and Ru360 treatment. The slopes of the respective linear regressions were statistically not different between control and mutant fibroblasts (**Figure 2 F**), indicating a disruption of the calcium buffering capacity when mitochondrial calcium uptake was blocked by Ru360. These results suggest that the reduced capacity of Miro1 mutant fibroblasts to buffer cytosolic calcium is due to impaired mitochondrial buffering.

This hypothesis was further strengthened by data resulting from the analysis of calcium-induced MiST, a mechanism which was recently identified as a pre-requisite of mitophagy and which is dependent on the ability of Miro1 to regulate calcium homeostasis [9]. Fibroblasts were stained with MitoTracker green FM and treated with the calcium ionophore ionomycin in order to increase cytosolic calcium levels. Independent of their genotype, all cells reacted to the ionomycin exposure with mitochondrial fragmentation as reflected by a decrease in the aspect ratios. However, in both Miro1-mutant fibroblast lines, we observed an increased fragmentation of the mitochondrial network compared to control fibroblasts (**Figure 2 H, I**). These results suggest that the impaired calcium buffering capacity of Miro1-mutant cells results in prolonged and elevated cytosolic calcium levels, which subsequently cause an increased induction of calcium-mediated mitochondrial fragmentation.

Decreased ER-mitochondrial contact sites in Miro1-mutant fibroblasts

Closely related to its function in cellular calcium homeostasis, Miro1 is also involved in the regulation of ER-mitochondria contact sites [19]. In light of the observed impaired mitochondrial calcium buffering in Miro1-mutant fibroblasts, we next studied the co-localization of the ER and mitochondria using MitoTracker deep red and ER-Tracker green (**Figure 3A**). We observed a significant reduction of ER-mitochondria contacts in both patient-derived fibroblast lines compared to control lines, when normalized to cell count (**Figure 3B**), ER area (**Figure 3C**) or mitochondria area (**Figure 3D**). Intriguingly, we also observed an overall reduction of ER area (**Figure 3E**) and mitochondrial area (**Figure 3F**) in Miro1-R272Q and R450C fibroblasts. These results were confirmed by immunocytochemistry of ER and mitochondrial marker proteins PDI and Tom20 (**Figure 3G**). Subsequent co-localization analysis showed a significant reduction of ER-mitochondria contacts in Miro1-mutant fibroblasts (**Figure 3H**) and ER area was likewise significantly reduced (**Figure 3I**), while mitochondria area showed a tendency to be reduced in Miro1-mutant fibroblasts compared to controls (**Figure 3J**).

Our results point to a reduction of ER-mitochondria contact sites in fibroblasts with mutations in Miro1.

Antioxidants and Redox Signaling
Mutations in *RHOT1* disrupt ER-mitochondria contact sites interfering with calcium homeostasis and mitochondrial dynamics in Parkinson's disease (DOI: 10.1089/ars.2018.7718)
This paper has been peer-reviewed and accepted for publication, but has yet to undergo copyediting and proof correction. The final published version may differ from this proof.

Mutant Miro1 protein leads to reduction of mitochondrial mass

Based on the reduced mitochondrial area observed during our microscopy analysis of ER-mitochondria contact sites (**Figure 3F**), we further investigated mitochondrial mass in Miro1-mutant fibroblasts. To this end, we performed Western blotting analyses of different mitochondrial marker proteins. First, we confirmed a reduction of Tom20 in the mutant fibroblasts (**Figure 4A, B**). In addition, we quantified the abundance of the mitochondrial matrix marker Hsp60 [20][21]. Indeed, Hsp60 protein levels were found to be significantly reduced in mutant compared to control fibroblasts (**Figure 4C, D**). Finally, we investigated the protein levels of Miro1 itself and also confirmed a reduction in fibroblasts expressing mutant Miro1 (**Figure 4E, F**). As both, the Miro1-R272Q and the Miro1-R450C mutant fibroblast lines were heterozygous, these results raised the question whether the observed mitochondrial phenotypes are due to a gain-of-function effect or due to the loss of Miro1 function. In order to answer this question, we generated a M17 cell model with stable knockdown of endogenous *RHOT1* and transient overexpression of the PD-associated Miro1 variants (**Suppl. Figure 1**). Western blot analyses revealed that knockdown of *RHOT1* alone (untransfected M17 cells + miRNA) had no effect on protein levels of Tom20 or the mitochondrial matrix marker MnSOD [20][21], whereas overexpression of Miro1-R272Q or Miro1-R450C, but not WT-Miro1, led to a significant reduction of Tom20 (**Figure 4G, H**) and MnSOD (**Figure 4I, J**), respectively. From these results, we concluded that the R272Q and the R450C mutations in Miro1 cause a toxic gain-of-function.

Mitochondrial turnover is increased in Miro1-mutant fibroblasts

Previous studies reported that the PINK1/Parkin-driven proteasomal degradation of Miro1 is part of the initial step of mitophagy [2][4][22][23][24]. Given the observed reduced levels of Miro1 protein and mitochondrial mass in Miro1-mutant cells (**Figure 4**), we were interested to investigate the underlying degradation pathways. Patient-derived fibroblasts were therefore treated with the proteasomal inhibitor MG132 and bafilomycinA_1, an inhibitor of the lysosomal degradation pathway. Western blot analysis showed an increase of Miro1 protein levels (**Figure 5A, B**) as well as Tom20 protein levels (**Figure 5C, D**) after MG132 treatment, but not after bafilomycinA_1 treatment, suggesting that both, Miro1 and

Tom20 are predominantly degraded by the proteasome. This result is in line with the literature, indicating that Miro1 and Tom20 are targeted by PINK1/Parkin for proteasomal degradation during mitophagy [20][21][22][23][24][25]. To further test this hypothesis, we assessed Parkin levels in patient-derived fibroblasts. FCCP treatment for 14 hours significantly decreased Parkin levels in control fibroblasts, suggesting an activation of mitophagy (**Figure 5 E, F**). By contrast, Parkin levels were already found to be significantly reduced at baseline conditions in both Miro1-mutant fibroblast lines (**Figure 5F**). These results, together with the reduction of mitochondrial mass (**Figure 4**), support that mitochondria undergo increased clearance in Miro1-mutant fibroblasts under basal conditions.

LC3-dependent autophagy is affected in Miro1-mutant fibroblasts

Since we observed reduced mitochondrial mass (**Figure 4**) and activation of mitochondrial clearance (**Figure 5**), we next analysed autophagy in immortalized Miro1-mutant and control fibroblasts. To assess autophagic flux, we treated cells with bafilomycinA_1. Western blot analysis revealed that LC3-II protein levels normalized to β-Actin [26], as well as the ratio of LC3-II to LC3-I protein levels increased significantly in control fibroblasts, but not in the Miro1-mutant fibroblast lines (Fig. **6A, B**), indicating a reduced capacity to enhance the autophagic flux. To further characterize the autophagy pathway and based on our findings of reduced ER-mitochondrial contact sites in cells expressing mutant Miro1, we stained fibroblasts with fluorescently labelled phosphatidylserine (18:1 NBD-PS). Phosphatidylserine (PS) is transferred at ER-mitochondria contact sites from the ER to mitochondria, where it is converted to phosphatidylethanolamine (PE). PE is then transferred through the ER-mitochondria contact sites back to the ER and contributes together with the cytosolic LC3-I to create autophagosomes (see **Figure 7F**). In this assay, the formation of autophagosomes is reflected by translocation of the 18:1 NBD-PS fluorescence signal from mitochondria to the cytosol [9][27](**Figure 6C**). FBS starvation for 2 hours induced autophagosome formation in control fibroblasts, while Miro1-mutant fibroblasts showed no increased autophagosome formation compared to the untreated condition (**Figure 6D**). To specifically analyse mitophagy, fibroblasts were transfected with mito-DsRed and eGFP-LC3 and subsequently treated with CCCP to induce mitophagy, or

Antioxidants and Redox Signaling
Mutations in *RHOT1* disrupt ER-mitochondria contact sites interfering with calcium homeostasis and mitochondrial dynamics in Parkinson's disease (DOI: 10.1089/ars.2018.7718)
This paper has been peer-reviewed and accepted for publication, but has yet to undergo copyediting and proof correction. The final published version may differ from this proof.

with bafilomycinA_1 in order to inhibit autophagy. Mitophagy was subsequently assessed by quantification of mitochondria co-localizing with LC3 puncta, which allowed us to analyse only those autophagosomes that are involved in mitochondrial degradation (**Figure 6E, F**)[26]. Under CCCP or bafilomycinA_1 treatment, the co-localization of mito-DsRed-labeled mitochondria and eGFP-LC3 puncta significantly increased in control fibroblasts, whereas no significant increase could be observed in Miro1-mutant fibroblasts, compared to baseline conditions (**Figure 6E**). Our results support the idea of already elevated mitophagy rates in the R272Q and R450C fibroblasts at baseline, as indicated by a higher frequency of mitochondria-LC3 co-localizing events in the untreated mutant cells compared to untreated control cells (**Figure 6E**). These results suggest that, while the total autophagosome formation under baseline conditions is not affected in Miro1-muant cells compared to controls, the capacity to further upregulate autophagosome formation is inhibited in those cells (**Figure 6D**). Furthermore, the created autophagosomes are involved in increase mitochondrial turnover, which likewise lacks the capacity for further upregulation under stress conditions (**Figure 6E**).

Mutations in Miro1 lead to increased LC3-independent autophagy and impaired energy metabolism

Our results suggest alterations of LC3-dependent autophagy in Miro1-mutant fibroblasts (**Figure 6**), significantly reduced mitochondrial mass (**Figure 3, 4**) and increased mitochondrial clearance (**Figure 5**). Therefore, we also investigated an alternative, LC3-independent clearance pathway, where autophagosomes are derived from the Golgi apparatus and their formation is mediated by Rab9 [28]. When analysing protein levels of Rab9 in cytosolic and mitochondrial fractions by Western blotting, we found that Rab9 levels were significantly reduced in mitochondrial fractions of Miro1-mutant fibroblasts compared to control fibroblasts (**Figure 7A, B**). In order to test whether these results were linked to autophagy, we treated fibroblasts with bafilomycinA_1. This experiment showed an increase in Rab9 levels after bafilomycinA_1 treatment in Miro1-mutant fibroblasts, but not in control cells (**Figure 7C, D**), suggesting a higher lysosomal turnover of Rab9. From these results, we concluded that mitochondrial degradation in Miro1-mutant fibroblasts is additionally driven by the Atg5/LC3-indipendent macroautophagy pathway.

Finally, since mitophagy and calcium homeostasis are closely linked to mitochondrial energy metabolism, we next sought to investigate the ATP production in our patient and control cultures. Measuring cellular ATP concentrations under baseline conditions showed significantly reduced steady-state-levels in both mutant fibroblast lines compared to control cells (**Figure 7E**).

Discussion

Increasing evidence supports a contribution of impaired energy metabolism and mitochondrial dynamics to the pathogenesis of monogenic and sporadic PD, i.e. for at least seven established PD genes (PINK1, Parkin, DJ-1, LRRK2, ATP13A2, SNCA, VPS35) a role in mitochondrial homeostasis and clearance has been described [29]. Within this context, the encoded proteins interact with other targets, which are potentially relevant to the pathogenesis of PD. One of these targets is Miro1, which has been shown to directly interact with PINK1 and Parkin [24]. Moreover, recent studies suggest a function of Miro1 together with LRRK2 in the regulation of damage-induced mitochondrial arrest [10]. The pathological relevance of Miro1 was supported by the lethality of new-born homozygous *RHOT1* knockout mice [30] and larvae of *dMiro* knockout flies [31].

Here, we describe for the first time phenotypes in fibroblasts derived from PD patients carrying mutations in *RHOT1*. These mutations lead to a decrease in ER-mitochondria contact sites, which consequently caused (i) impaired cellular calcium homeostasis and (ii) increased calcium-induced mitochondrial fragmentation. These phenotypes ultimately (iii) induce mitochondrial clearance. However, the LC3-dependent formation of autophagosomes lacks the capacity to further promote mitophagy under stress conditions. Mitophagy is therefore additionally driven by LC3-independent autophagy via Rab9, resulting in (iv) reduced mitochondrial mass in Miro1-mutant cells (see overview **Figure 7F**).

The herein described Miro1-muant fibroblast lines displayed strikingly similar phenotypes, although the R272Q and R450C mutations are located in different domains of the protein, i.e. the EF-hand and the C-terminal GTPase domain. Both domains have been shown to form a unique side-by-side 3D structure that facilitates their close interplay [13], which is crucial for the calcium sensing ability of Miro1 [3][7][8][13][19]. In light of these previous

Antioxidants and Redox Signaling
Mutations in *RHOT1* disrupt ER-mitochondria contact sites interfering with calcium homeostasis and mitochondrial dynamics in Parkinson's disease (DOI: 10.1089/ars.2018.7718)
This paper has been peer-reviewed and accepted for publication, but has yet to undergo copyediting and proof correction. The final published version may differ from this proof.

reports, we conclude from our data that both mutations in Miro1 disrupt the proteins calcium-sensing function.

The importance of cellular calcium regulation at ER-mitochondrial contact sites for the function and survival of neuronal cells was recently highlighted by studies in *drosophila*. Lee and colleagues identified Miro1 as regulator of calcium transporters at the ER-mitochondrial contact sites, a function that was independent of Miro1's role in mitochondrial transport. Inactive Miro1 was found to cause mitochondrial calcium depletion and metabolic dysfunction, leading to impaired neuronal stem cell development in flies [32].

ER-mitochondrial contact sites not only regulate cytosolic and mitochondrial calcium homeostasis, but also autophagy. Within this mechanism, Miro1 acts as receptor at the outer mitochondrial membrane to sense cytosolic calcium levels. Upon increase of calcium levels, Miro1 mediates Drp1/Fis1-independent mitochondrial fragmentation, also called MiST, and subsequent mitophagy. Disruption of the calcium-binding ability of Miro1 leads to impaired regulation of calcium homeostasis and mitophagy [9]. Indeed this is in line with our findings of impaired cellular calcium homeostasis and increased calcium-induced mitochondrial fragmentation in Miro1-mutant fibroblasts.

Calcium dyshomeostasis is commonly observed in neurological diseases and recently, the regulation of calcium homeostasis and autophagy at ER-mitochondrial contact sites came into focus in the context of PD. *Drosophila* expressing a PINK1 loss-of-function mutation or the PD-associated mutation G2019S in LRRK2 displayed impaired calcium homeostasis at ER-mitochondrial contact sites, which resulted in mitochondrial dysfunction and loss of dopaminergic neurons, and Miro1 was identified as key player in this process [33]. Also Parkin was found to be involved in the regulation of ER-mitochondria contact sites. Mirroring the phenotypes found in Miro1-mutant fibroblasts in this study, Cali and colleagues showed that knockdown of Parkin in SH-SY5Y cells results in mitochondrial fragmentation, alterations of mitochondrial calcium transients and a reduction of ER-mitochondria contact sites. They concluded that, just like Miro1, Parkin is involved in the maintenance of the mitochondrial network integrity via regulation of the ER-mitochondria contact sites and calcium transfer between both organelles [34]. Similar observations were made in S2R+ *drosophila* cells or mouse embryonic fibroblasts with knockdown of Parkin

and fibroblasts derived from a PD patient with compound heterozygous mutant Parkin (R275W, exon 3 deletion) [35]. The results of this study suggested that Parkin regulates the function of ER-mitochondrial contact sites by ubiquitination of Mfn2 [35]. Also, loss of function models of Parkin and PINK1 in fly ventral neurons and human iPSC-derived hypothalamic neurons resulted in alterations of ER-mitochondrial connections and a thereof resulting deregulation of phosphatidylserine transfer, in turn leading to impaired production of neuropeptide-containing vesicles. The resulting changes of neuropeptidergic neurotransmission caused impaired sleep patterns in the PD fly model [36]. It is worth noting that some studies found an increase of ER-mitochondria contact sites, where others found a decrease, caused by impaired PINK1, Parkin or Miro1 function. These differences seem to be cell type-specific, as knockdown of Parkin in non-neuronal, mitotic cells leads to a reduction of ER-mitochondrial connections [34][35], but knockdown of PINK1, Parkin or Miro1 in neurons was associated with increased contact sites [36][33].

In conclusion, our results support an important role of Miro1 in cellular calcium homeostasis and autophagy, highlighting *RHOT1* as candidate gene in the pathogenesis of neurodegenerative disorders like PD.

Materials and Methods

Screening for PD patients with mutations in RHOT1

DNA was obtained from 752 German PD patients (average age of onset of 59.4 ± 13.2 years, average age of sample collection of 65.7 ± 10.2 years) and 282 age-matched healthy control individuals (average age 72 ± 4.4 years) from the MEMO study [37]. Informed consent was obtained from patients and approved by the Ethics Committee of the Medical faculty and the University Hospital Tübingen, Germany. Ninety-two samples of healthy individuals from the TREND study (www.trend-studie.de) [38] served as additional control cohort. PCR amplification of exons 2 - 21 of *RHOT1* (Ensembl.org: RHOT1-002, ENST00000358365) from whole blood DNA samples was performed using the primers listed in (**Suppl.1**; Metabion, Germany). SYBR Green on the LightCycler 480 High Resolution Master (Roche) and subsequent High Resolution Melting Analysis (HRMA) were used for mutation screening. Potential mutation sites were validated by Sanger sequencing.

Genotyping of additional cohorts for the herein described *RHOT1* variants was performed by the central genotyping core at the Institute of Human Genetics, Helmholtz Zentrum

Antioxidants and Redox Signaling
Mutations in *RHOT1* disrupt ER-mitochondria contact sites interfering with calcium homeostasis and mitochondrial dynamics in Parkinson's disease (DOI: 10.1089/ars.2018.7718)
This paper has been peer-reviewed and accepted for publication, but has yet to undergo copyediting and proof correction. The final published version may differ from this proof.

München, Neuherberg, Germany, using a matrix-assisted laser desorption/ionization time-of-flight (MALDI-TOF) mass spectrometry on a MassArray system (Agena Bioscience, San Diego, CA, USA). We included 662 age-matched control individuals from the KORA cohort (KORA, Cooperative Research in the Region of Augsburg, Germany) and 1238 PD patients of German origin [14]. The genotyping core was blinded to case-control status. Cleaned extension products were analyzed by a mass spectrometer (Bruker Daltonik, USA) and peaks identified using the MassArray Typer 4.0.2.5 software (Agena Bioscience). The average call rate of the variants was 97%.

In silico prediction of pathogenic effects of RHOT1 mutations

ANNOVAR [39] was used to annotate the *RHOT1* mutations using the dbNSFP database version 3.0 [40]. The following prediction tools were used: SIFT [41], PolyPhen2 [42], Mutation Taster [43], Mutation assessor [44], FATHMM [45], LRT (Likelihood ratio test; http://www.genetics.wustl.edu/jflab/lrt_query.html; [46], radial SVM and LR pred [47].

3D modelling of human Miro1

A homology model for human Miro1 was derived from the crystal structure of the drosophila ortholog (PDB: 4COJ) using the I-TASSER software with default parameters [48]. To visualize the mutations in the homology model, the wildtype residues were replaced by the rotamers with the highest probability using the "Rotamers" tool in the software Chimera [49], and an energy minimization was applied to these residues with standard settings.

Genetic burden analysis for RHOT1

We used the gnomAD browser to analyse the mutational burden for *RHOT1* (https://gnomad.broadinstitute.org/gene/ENSG00000126858) [50]. Z-scores for missense and synonymous variants were calculated from numbers of observed over expected variants and positive z-scores indicate that there are fewer variants than statistically expected. The observed/expected score (o/e) and the pLI score indicate the tolerance of a gene against Loss-of-Function variants. Low o/e values indicate that the gene is under

stronger selection. The closer to 1, the less tolerant the gene is against LoF variants and genes with pLI >= 0.9 are considered to be extremely intolerant to LoF variants [50].

Antioxidants and Redox Signaling
Mutations in *RHOT1* disrupt ER-mitochondria contact sites interfering with calcium homeostasis and mitochondrial dynamics in Parkinson's disease (DOI: 10.1089/ars.2018.7718)
This paper has been peer-reviewed and accepted for publication, but has yet to undergo copyediting and proof correction. The final published version may differ from this proof.

Immortalization and culture of fibroblasts

Skin biopsies were obtained from two female PD patients at the age of 78 (Miro1-R272Q) or 54 (Miro1-R450C). Control fibroblasts were gender- and age-matched to patient-derived fibroblasts and obtained from the Neuro-Biobank of the University of Tübingen, Germany. Informed written consent of all individuals was obtained at the University Hospital Tübingen, Germany. Fibroblasts were immortalized with a pLenti-III-SV40 construct (Applied Biological Materials Inc., Richmond, Canada, Cat. G203). All fibroblasts were grown in DMEM+/+ medium (containing 4.5 g/L D-Glucose, 15 % FBS, 1 % Pen/Strep; Thermo Fisher Scientific, Braunschweig, Germany). Cells were tested for Mycoplasma contamination on a monthly base using the Plasmo Test™ Detection Kit (InvivoGen).

Generation of M17 model with knockdown of endogenous RHOT1 and overexpression of Miro1

The human neuroblastoma cell line M17 was grown in DMEM/F12+/+ medium (DMEM/Ham's-F12 + 15 % FBS + 1 % L-Glutamine + 1% non-essential amino acids + 1 % Pen/Strep). Cells were split using Trypsin-EDTA (0,05 %), phenol red (Thermo Fisher Scientific, Braunschweig, Germany). We introduced a stable knockdown of endogenous *RHOT1* employing the BLOCK-iT Inducible Pol II miR RNAi Expression Vector Kit (Invitrogen GmbH, Karlsruhe, Germany) according to the manufacturer's protocol. We designed the following single-stranded nucleotide oligomers, targeting different regions of *RHOT1:* miRNA-524 (top strand: 5' TGC TGT TTA TGA GAG GAA TCC ATC GAG TTT TGG CCA CTG ACT GAC TCG ATG GAC CTC TCA TAA A 3'; bottom strand: 5'CCT GTT TAT GAG AGG TCC ATC GAG TCA GTC AGT GGC CAA AAC TCG ATG GAT TCC TCT CAT AAA C 3'); miRNA-1335 (top strand: 5' TGC TGT AAA TAA GTC GTG AGC GTC CAG TTT TGG CCA CTG ACT GAC TGG ACG CTC GAC TTA TTT A 3'; bottom strand: 5' CCT GTA AAT AAG TCG AGC GTC CAG TCA GTC AGT GGC CAA AAC TGG ACG CTC ACG ACT TAT TTA C 3'); or miRNA-2471 (top strand: 5' TGC TGT ATG CTA GCC AAT ACT GCA GTG TTT TGG CCA CTG ACT GAC ACT GCA GTT GGC TAG CAT A 3'; bottom strand: 5' CCT GTA TGC TAG CCA ACT GCA GTG TCA GTC AGT GGC

Antioxidants and Redox Signaling
Mutations in *RHOT1* disrupt ER-mitochondria contact sites interfering with calcium homeostasis and mitochondrial dynamics in Parkinson's disease (DOI: 10.1089/ars.2018.7718)
This paper has been peer-reviewed and accepted for publication, but has yet to undergo copyediting and proof correction. The final published version may differ from this proof.

CAA AAC ACT GCA GTA TTG GCT AGC ATA C 3'). The oligomers were cloned into the pcDNA6.2-GW/EmGFP-miR vector provided by the kit and transfected into M17 cells. Cells were subsequently selected and continuously maintained with 6 µg/mL Blasticidin S HCl (Invitrogen GmbH, Karlsruhe, Germany). Knockdown of endogenous *RHOT1* was verified by Western blot analysis (**Suppl. Figure 1A**). For our experiments, we choose the miRNA-2471, which showed the most efficient knockdown. As miRNA-2471 was designed to target the 5'UTR of *RHOT1* instead of the open reading frame, we were able to overexpress recombinant Miro1, using *RHOT1* variants cloned into pcDNA3.1/V5-HisA (Invitrogen). M17 cells were transiently transfected with these constructs using *Trans*IT®-2020 transfection reagent (Mirus Bio, MIR 5400). Overexpression was also verified by Western blot analysis (**Suppl. Figure 1B, C**).

Overexpression of Parkin in SH-SY5Y cells

Neuroblastoma (SH-SY5Y) cells stably overexpressing Parkin were generated using lentiviral particles. To produce Parkin-expressing lentiviral particles, a cassette consisting of the open reading frame of the Parkin gene (NM_004562.3), the IRES sequence, and the Puromycin resistance gene were cloned into pLenti4/V5-DEST (ThermoFisher) plasmid (pLenti4-TH-IRES-Puromycin). Next, 293FT cells were cotransfected with pLenti-Parkin-IRES-Puromycin and the ViraPowerTM Packaging Mix (ThermoFisher) to generate a lentiviral stock. SH-SY5Y cells were transduced using lentiviral particles for 48 h and subsequently selected by using 2 µg/ml Puromycin (ThermoFisher) for 48 h.

SDS-PAGE and Western blot analysis

Fibroblasts were lysed in RIPA buffer containing 1x complete protease inhibitor (Roche, Germany). Western blot analysis was performed with antibodies against LC3-I/II (Cell Signaling, 2775), Hsp60 (Cell Signaling, 4870), Tom20 (Santa Cruz Biotechnologies, sc-17764), Rab9 (Santa Cruz Biotechnologies, sc-74482), MnSOD (Abcam, ab13533), anti-V5 (Sigma Aldrich, R960-25; Novex, R96125) and β-Actin (Thermo Scientific, MA1-744). Mitochondrial fractionation was performed as described before [51].

Antioxidants and Redox Signaling
Mutations in *RHOT1* disrupt ER-mitochondria contact sites interfering with calcium homeostasis and mitochondrial dynamics in Parkinson's disease (DOI: 10.1089/ars.2018.7718)
This paper has been peer-reviewed and accepted for publication, but has yet to undergo copyediting and proof correction. The final published version may differ from this proof.

Live cell imaging

Fibroblasts were seeded into Nunc™ Lab-Tek™ Chamber slides (Thermo Fisher Scientific, Braunschweig, Germany) for imaging. Live cell imaging was performed with a Live Cell Microscope Axiovert 2000 with spinning disc, plan-apochromate objectives and Hamamatsu camera C11440 (Carl Zeiss Microimaging GmbH, Jena, Germany) in a humidified atmosphere containing 5 % CO_2 at 37°C.

For calcium imaging, fibroblasts were stained with 0.1 µM MitoTracker® deep red FM (Thermo Fisher Scientific, Braunschweig, Germany) in DMEM +/+ and Fluo4-AM (Thermo Fisher Scientific, Braunschweig, Germany). During imaging, Fluo4-AM was present in the medium at a 1:1 (v/v) dilution. During imaging, cells were treated with 1 µM thapsigargin (Sigma-Aldrich, Munich, Germany). To test for the involvement of mitochondria in cytosolic calcium regulation, we incubated the cells with 10 µM Ru360 (Sigma-Aldrich, Munich, Germany). After treatment, time-laps imaging was continued for 10 min and images were acquired every 2 seconds.

For analysis of co-localization of mitochondria and LC3 puncta, immortalized fibroblasts were transfected with mito-DsRed [52] and eGFP-LC3 [53] using TransIT-2020 transfection reagent (Mirus Bio LLC, Madison, USA). Cells were then treated with 25 µM CCCP or 10 nM bafilomycinA_1 for 2 hours or 6 hours, respectively.

For analysis of autophagosome formation, cells were stained with 0.2 mM 18:1 NBD-PS (Sigma-Aldrich, 810198C) for 30 min at 37°C. Cells were subsequently starved in medium without FBS for 2 hours.

For co-localization analysis of mitochondria and ER, native fibroblasts were stained with 0.1 µM MitoTracker® deep red FM and 1 µM ER-tracker green (Thermo Fisher Scientific, Braunschweig, Germany) and imaged using the 368 nm or 488 nm laser.

For analysis of calcium-induced mitochondrial fragmentation, immortalized fibroblasts were stained with 0.1 µM MitoTracker® green FM (Thermo Fisher Scientific, Braunschweig, Germany) for 45 min at 37°C. After 1 min of imaging, cells were treated with 20 µM ionomycin (Sigma-Aldrich, Munich, Germany) and imaging was continued for 20 min.

All image analysis was done with MATLAB or ImageJ.

Antioxidants and Redox Signaling
Mutations in *RHOT1* disrupt ER-mitochondria contact sites interfering with calcium homeostasis and mitochondrial dynamics in Parkinson's disease (DOI: 10.1089/ars.2018.7718)
This paper has been peer-reviewed and accepted for publication, but has yet to undergo copyediting and proof correction. The final published version may differ from this proof.

Immunofluorescence stainings

For co-localization analysis of mitochondria and ER, native fibroblasts were fixed with 4% PFA for 15 min and then labelled with antibodies against Tom20 (Santa Cruz Biotechnologies, sc-17764, dilution 1:500; secondary antibody: goat anti-mouse Alexa Fluor 647, Life Technologies, A-21235, dilution 1:1000) and PDI (Cell Signalling Technology, 2446S, dilution 1:1000; secondary antibody: goat anti-rabbit Alexa Fluor 488, Life Technologies, A-1000, dilution 1:1000).

Measurement of ATP level

Steady-state ATP levels were measured in immortalized fibroblasts (n = 500.000 cells) grown under standard conditions. The quantification of total ATP levels was performed with the ATP Bioluminescence Assay Kit CLS II (Roche) according to the manufacturer's protocol in 96 well plates (Greiner bio-one). The luminescence signal was detected with the Microplate Reader infinite M200Pro (TECAN).

Statistics

Statistical significance was determined using GraphPad Prism 6.0 software. Statistical tests and P-values are indicated in the figure legends. To account for the small sample size used in this study, we employed non-parametric tests throughout. All experiments were independently repeated at least three times (n represents the number of independent, biological replicates).

Author contributions

Research project: Conception: RK, DG, JCF, DR, AS, AFH, AG; Organization: DG, RK, Execution: DG, CB, MEB, FM, JB, JG, DS, MS, PL, EG, PM, KSD, AR; Statistical analysis: Design and Execution: DG, MEB, PA, EG, PM, KSD, PL; Review and Critique: AS, AFH, PA, EG, PM, KSD, DR; Manuscript: Writing: DG, AG; Review and Critique: DR, AS, AFH, PL, PA, EG, PM, KSD, JCF, AG, RK.

Acknowledgements

We thank all patients and control individuals for their commitment and support for research. The KORA research platform (KORA, Cooperative Research in the Region of Augsburg) was initiated and financed by the Helmholtz Zentrum München - German Research Center for Environmental Health and funded by the German Federal Ministry of Education and Research and by the State of Bavaria, Germany. KORA research was supported within the Munich Center of Health Sciences (MC Health), Ludwig-Maximilians-Universität, as part of LMUinnovativ. The control fibroblasts were obtained from the Neuro-Biobank of the University of Tübingen, Germany (https://www.hih-tuebingen.de/en/about-us/core-facilities/biobank/). This biobank is supported by the local University, the Hertie Institute and the DZNE. The Miro1-WT/myc in the pRK5-myc vector was a kind gift of Prof. Pontus Aspenström, Karolinska Institute, Sweden.

Antioxidants and Redox Signaling
Mutations in *RHOT1* disrupt ER-mitochondria contact sites interfering with calcium homeostasis and mitochondrial dynamics in Parkinson's disease (DOI: 10.1089/ars.2018.7718)
This paper has been peer-reviewed and accepted for publication, but has yet to undergo copyediting and proof correction. The final published version may differ from this proof.

Antioxidants and Redox Signaling

Mutations in *RHOT1* disrupt ER-mitochondria contact sites interfering with calcium homeostasis and mitochondrial dynamics in Parkinson's disease (DOI: 10.1089/ars.2018.7718)
This paper has been peer-reviewed and accepted for publication, but has yet to undergo copyediting and proof correction. The final published version may differ from this proof.

List of Abbreviations

ER	endoplasmic reticulum
LoF	loss-of-function
MCU	mitochondrial calcium uniporter
MiST	mitochondrial shape transition
PD	Parkinson's disease
PE	phosphatidylethanolamine
PS	phosphatidylserine

Conflict of Interest:

Authors declare no conflict of interest.

Funding sources for this study:

RK has received research grants from Fonds National de la Recherche de Luxembourg (PEARL [FNR/P13/6682797/Krüger] and NCER-PD), the German Research Council (KR2119/8-1), the European Union's Horizon2020 research and innovation program (WIDESPREAD; CENTRE-PD; grant agreement no. 692320) and the Federal Ministry for Education and Research (BMBF; Mito-PD 031 A 430 A). RK, AG, EG, MS and PM received funding from the CORE programme of the Fonds National de Recherche de Luxembourg (FNR, MiRisk-PD, C17/BM/11676395). AS was supported by the Fonds National de la Recherche through the C14/BM/7975668/CaSCAD grant, and the National Biomedical Computation Resource (NBCR) through the NIH P41 GM103426 grant from the National Institutes of Health. EG received support by the Fonds Nationale de la Recherche, Luxembourg, as part of the project MitoPD, under the auspices of the bilateral e:Med program by the German Federal Ministry of Education and Research and the FNR (INTER/BMBF/13/04). KSD was supported by the German Research Council (DI 1386/2-1). JCF acknowledges funding from the German Research Council, German Federal Ministry of Education and Research (BMBF) support code 031 A 430 A, DZNE, the University of Tubingen and the EU Joint Programme - Neurodegenerative Disease Research (JPND) project. AG received funding from the Fonds National de la Recherche within the ATTRACT programme (FNR, Model IPD, FNR9631103). RK, EG and PM received funding from the European Union's Joint Program-Neurodegenerative Diseases (JPND; COURAGE-PD). AR was supported by the DFG (FOR2488).

Financial Disclosures of all authors (for the preceding 12 months)

RK received honoraria/ travel grants from Abbvie, Zambon and Medtronic and participated as site-PI for industry sponsored clinical trials without receiving additional honoraria.

Antioxidants and Redox Signaling
Mutations in *RHOT1* disrupt ER-mitochondria contact sites interfering with calcium homeostasis and mitochondrial dynamics in Parkinson's disease (DOI: 10.1089/ars.2018.7718)
This paper has been peer-reviewed and accepted for publication, but has yet to undergo copyediting and proof correction. The final published version may differ from this proof.

Antioxidants and Redox Signaling
Mutations in *RHOT1* disrupt ER-mitochondria contact sites interfering with calcium homeostasis and mitochondrial dynamics in Parkinson's disease (DOI: 10.1089/ars.2018.7718)
This paper has been peer-reviewed and accepted for publication, but has yet to undergo copyediting and proof correction. The final published version may differ from this proof.

References

1. Wang X, Schwarz TL. The Mechanism of Ca2+-Dependent Regulation of Kinesin-Mediated Mitochondrial Motility. Cell [Internet]. Elsevier Inc.; 2009;136:163–74. Available from: http://dx.doi.org/10.1016/j.cell.2008.11.046

2. Wang X, Winter D, Ashrafi G, Schlehe J, Wong YL, Selkoe D, et al. PINK1 and Parkin target miro for phosphorylation and degradation to arrest mitochondrial motility. Cell [Internet]. Elsevier Inc.; 2011;147:893–906. Available from: http://dx.doi.org/10.1016/j.cell.2011.10.018

3. Chang KT, Niescier RF, Min K-T. Mitochondrial matrix Ca2+ as an intrinsic signal regulating mitochondrial motility in axons. Proc Natl Acad Sci [Internet]. 2011;108:15456–61. Available from: http://www.pnas.org/cgi/doi/10.1073/pnas.1106862108

4. Weihofen A, Thomas KJ, Ostaszewski BL, Cookson MR, Selkoe DJ. Pink1 Forms a Multiprotein Complex with Miro and Milton, Linking Pink1 Function to Mitochondrial Trafficking †. Biochemistry [Internet]. 2009;48:2045–52. Available from: http://pubs.acs.org/doi/abs/10.1021/bi8019178

5. Vlahou G, Eliáš M, von Kleist-Retzow JC, Wiesner RJ, Rivero F. The Ras related GTPase Miro is not required for mitochondrial transport in Dictyostelium discoideum. Eur J Cell Biol. 2011;90:342–55.

6. MacAskill AF, Brickley K, Stephenson FA, Kittler JT. GTPase dependent recruitment of Grif-1 by Miro1 regulates mitochondrial trafficking in hippocampal neurons. Mol Cell Neurosci [Internet]. Elsevier Inc.; 2009;40:301–12. Available from: http://dx.doi.org/10.1016/j.mcn.2008.10.016

7. Saotome M, Safiulina D, Szabadkai G, Das S, Fransson A, Aspenstrom P, et al. Bidirectional Ca2+-dependent control of mitochondrial dynamics by the Miro GTPase. Proc Natl Acad Sci [Internet]. 2008;105:20728–33. Available from: http://www.pnas.org/cgi/doi/10.1073/pnas.0808953105

8. Stephen T-L, Higgs NF, Sheehan DF, Al Awabdh S, Lopez-Domenech G, Arancibia-Carcamo IL, et al. Miro1 Regulates Activity-Driven Positioning of Mitochondria within Astrocytic Processes Apposed to Synapses to Regulate Intracellular Calcium Signaling. J Neurosci [Internet]. 2015;35:15996–6011. Available from: http://www.jneurosci.org/cgi/doi/10.1523/JNEUROSCI.2068-15.2015

9. Nemani N, Carvalho E, Tomar D, Dong Z, Ketschek A, Breves SL, et al. MIRO-1 Determines Mitochondrial Shape Transition upon GPCR Activation and Ca2+Stress. Cell Rep. 2018;1005–19.

10. Hsieh CH, Shaltouki A, Gonzalez AE, Bettencourt da Cruz A, Burbulla LF, St. Lawrence E, et al. Functional Impairment in Miro Degradation and Mitophagy Is a Shared Feature in Familial and Sporadic Parkinson's Disease. Cell Stem Cell. 2016;19:709–24.

11. Hsieh C-H, Shaltouki A, Gonzalez AE, Bettencourt da Cruz A, Burbulla LF, St Lawrence E, et al. Functional Impairment in Miro Degradation and Mitophagy Is a Shared Feature in Familial and Sporadic Parkinson's Disease. Cell Stem Cell [Internet]. 2016;19:709–24. Available from: http://linkinghub.elsevier.com/retrieve/pii/S1934590916302491

12. Anvret A, Ran C, Westerlund M, Sydow O, Willows T, Olson L, et al. Genetic Screening of the Mitochondrial Rho GTPases MIRO1 and MIRO2 in Parkinson's Disease. Open Neurol J [Internet]. 2012;6:1–5. Available from: http://www.pubmedcentral.nih.gov/articlerender.fcgi?artid=3322431&tool=pmcentrez&rendertype=abstract%5Cnhttp://benthamopen.com/ABSTRACT/TONEUJ-6-1%5Cnhttp://www.ncbi.nlm.nih.gov/pubmed/22496713%5Cnhttp://www.pubmedcentral.nih.gov/articlerender.fcgi?artid=

13. Klosowiak JL, Focia PJ, Chakravarthy S, Landahl EC, Freymann DM, Rice SE. Structural coupling of the EF hand and C-terminal GTPase domains in the mitochondrial protein Miro. EMBO Rep [Internet]. Nature Publishing Group; 2013;14:968–74. Available from: http://dx.doi.org/10.1038/embor.2013.151

14. Wüst R, Maurer B, Hauser K, Woitalla D, Sharma M, Krüger R. Mutation analyses and association studies to assess the role of the presenilin-associated rhomboid-like gene in Parkinson's disease. Neurobiol Aging [Internet]. 2016;39:217.e13-5. Available from: http://www.ncbi.nlm.nih.gov/pubmed/26778534

15. Treiman M, Caspersen C, Christensen SB. A tool coming of age: thapsigargin as an inhibitor of sarco-endoplasmic reticulum Ca(2+)-ATPases. Trends Pharmacol Sci [Internet]. 1998;19:131–5. Available from: http://www.ncbi.nlm.nih.gov/pubmed/9612087

16. Parekh AB, Putney JW. Store-operated calcium channels. Physiol Rev [Internet]. 2005;85:757–810. Available from: http://www.ncbi.nlm.nih.gov/pubmed/15788710

Antioxidants and Redox Signaling
Mutations in *RHOT1* disrupt ER-mitochondria contact sites interfering with calcium homeostasis and mitochondrial dynamics in Parkinson's disease (DOI: 10.1089/ars.2018.7718)
This paper has been peer-reviewed and accepted for publication, but has yet to undergo copyediting and proof correction. The final published version may differ from this proof.

17. Vaccaro V, Devine MJ, Higgs NF, Kittler JT. Miro1-dependent mitochondrial positioning drives the rescaling of presynaptic Ca 2+ signals during homeostatic plasticity. EMBO Rep [Internet]. 2017;18:231–40. Available from: http://embor.embopress.org/lookup/doi/10.15252/embr.201642710

18. Kirichok Y, Krapivinsky G, Clapham DE. The mitochondrial calcium uniporter is a highly selective ion channel. Nature [Internet]. 2004;427:360–4. Available from: http://www.ncbi.nlm.nih.gov/pubmed/14737170

19. Kornmann B, Osman C, Walter P. The conserved GTPase Gem1 regulates endoplasmic reticulum-mitochondria connections. Proc Natl Acad Sci [Internet]. 2011;108:14151–6. Available from: http://www.pnas.org/cgi/doi/10.1073/pnas.1111314108

20. Rakovic A, Ziegler J, Mårtensson CU, Prasuhn J, Shurkewitsch K, König P, et al. PINK1-dependent mitophagy is driven by the UPS and can occur independently of LC3 conversion. Cell Death Differ [Internet]. 2018; Available from: http://www.ncbi.nlm.nih.gov/pubmed/30375512

21. Chan NC, Salazar AM, Pham AH, Sweredoski MJ, Kolawa NJ, Graham RLJ, et al. Broad activation of the ubiquitin-proteasome system by Parkin is critical for mitophagy. Hum Mol Genet [Internet]. 2011;20:1726–37. Available from: http://www.ncbi.nlm.nih.gov/pubmed/21296869

22. Liu S, Sawada T, Lee S, Yu W, Silverio G, Alapatt P, et al. Parkinson's disease-associated kinase PINK1 regulates miro protein level and axonal transport of mitochondria. PLoS Genet. 2012;8:15–7.

23. Sarraf SA, Raman M, Guarani-Pereira V, Sowa ME, Huttlin EL, Gygi SP, et al. Landscape of the PARKIN-dependent ubiquitylome in response to mitochondrial depolarization. Nature [Internet]. 2013;496:372–6. Available from: http://www.nature.com/articles/nature12043

24. Birsa N, Norkett R, Wauer T, Mevissen TET, Wu HC, Foltynie T, et al. Lysine 27 ubiquitination of the mitochondrial transport protein miro is dependent on serine 65 of the parkin ubiquitin ligase. J Biol Chem. 2014;289:14569–82.

25. Yoshii SR, Kishi C, Ishihara N, Mizushima N. Parkin mediates proteasome-dependent protein degradation and rupture of the outer mitochondrial membrane. J Biol Chem [Internet]. 2011;286:19630–40. Available from: http://www.ncbi.nlm.nih.gov/pubmed/21454557

26. Klionsky DJ, Abdelmohsen K, Abe A, Abedin MJ, Abeliovich H, Arozena AA, et al. Guidelines for the use and interpretation of assays for monitoring autophagy (3rd edition). Autophagy. 2016;12:1–222.

27. Hailey DW, Rambold AS, Satpute-Krishnan P, Mitra K, Sougrat R, Kim PK, et al. Mitochondria supply membranes for autophagosome biogenesis during starvation. Cell [Internet]. 2010;141:656–67. Available from: http://www.ncbi.nlm.nih.gov/pubmed/20478256

28. Nishida Y, Arakawa S, Fujitani K, Yamaguchi H, Mizuta T, Kanaseki T, et al. Discovery of Atg5/Atg7-independent alternative macroautophagy. Nature [Internet]. 2009;461:654–8. Available from: http://www.ncbi.nlm.nih.gov/pubmed/19794493

29. Larsen SB, Hanss Z, Krüger R. The genetic architecture of mitochondrial dysfunction in Parkinson's disease. Cell Tissue Res [Internet]. 2018; Available from: http://www.ncbi.nlm.nih.gov/pubmed/29372317

30. Nguyen TT, Oh SS, Weaver D, Lewandowska A, Maxfield D, Schuler M-H, et al. Loss of Miro1-directed mitochondrial movement results in a novel murine model for neuron disease. Proc Natl Acad Sci [Internet]. 2014;111:E3631–40. Available from: http://www.pnas.org/cgi/doi/10.1073/pnas.1402449111

31. Guo X, Macleod GT, Wellington A, Hu F, Panchumarthi S, Schoenfield M, et al. The GTPase dMiro is required for axonal transport of mitochondria to drosophila synapses. Neuron. 2005;47:379–93.

32. Lee S, Lee K-S, Huh S, Liu S, Lee D-Y, Hong SH, et al. Polo Kinase Phosphorylates Miro to Control ER-Mitochondria Contact Sites and Mitochondrial Ca 2+ Homeostasis in Neural Stem Cell Development. Dev Cell [Internet]. Elsevier Inc.; 2016;37:174–89. Available from: http://dx.doi.org/10.1016/j.devcel.2016.03.023

Antioxidants and Redox Signaling
Mutations in *RHOT1* disrupt ER-mitochondria contact sites interfering with calcium homeostasis and mitochondrial dynamics in Parkinson's disease (DOI: 10.1089/ars.2018.7718)
This paper has been peer-reviewed and accepted for publication, but has yet to undergo copyediting and proof correction. The final published version may differ from this proof.

33. Lee K-S, Huh S, Lee S, Wu Z, Kim A-K, Kang H-Y, et al. Altered ER-mitochondria contact impacts mitochondria calcium homeostasis and contributes to neurodegeneration in vivo in disease models. Proc Natl Acad Sci U S A [Internet]. 2018;115:E8844–53. Available from: http://www.ncbi.nlm.nih.gov/pubmed/30185553

34. Calì T, Ottolini D, Negro A, Brini M. Enhanced parkin levels favor ER-mitochondria crosstalk and guarantee Ca(2+) transfer to sustain cell bioenergetics. Biochim Biophys Acta [Internet]. 2013;1832:495–508. Available from: http://www.ncbi.nlm.nih.gov/pubmed/23313576

35. Basso V, Marchesan E, Peggion C, Chakraborty J, von Stockum S, Giacomello M, et al. Regulation of ER-mitochondria contacts by Parkin via Mfn2. Pharmacol Res [Internet]. 2018;138:43–56. Available from: http://www.ncbi.nlm.nih.gov/pubmed/30219582

36. Valadas JS, Esposito G, Vandekerkhove D, Miskiewicz K, Deaulmerie L, Raitano S, et al. ER Lipid Defects in Neuropeptidergic Neurons Impair Sleep Patterns in Parkinson's Disease. Neuron [Internet]. 2018;98:1155-1169.e6. Available from: http://www.ncbi.nlm.nih.gov/pubmed/29887339

37. Burbulla LF, Schelling C, Kato H, Rapaport D, Woitalla D, Schiesling C, et al. Dissecting the role of the mitochondrial chaperone mortalin in Parkinson's disease: Functional impact of disease-related variants on mitochondrial homeostasis. Hum Mol Genet. 2010;19:4437–52.

38. Hobert MA, Niebler R, Meyer SI, Brockmann K, Becker C, Huber H, et al. Poor trail making test performance is directly associated with altered dual task prioritization in the elderly--baseline results from the TREND study. PLoS One [Internet]. 2011;6:e27831. Available from: http://www.ncbi.nlm.nih.gov/pubmed/22114705

39. Wang K, Li M, Hakonarson H. ANNOVAR: functional annotation of genetic variants from high-throughput sequencing data. Nucleic Acids Res [Internet]. 2010;38:e164. Available from: http://www.ncbi.nlm.nih.gov/pubmed/20601685

40. Liu X, Wu C, Li C, Boerwinkle E. dbNSFP v3.0: A One-Stop Database of Functional Predictions and Annotations for Human Nonsynonymous and Splice-Site SNVs. Hum Mutat [Internet]. 2016;37:235–41. Available from: http://www.ncbi.nlm.nih.gov/pubmed/26555599

Antioxidants and Redox Signaling
Mutations in *RHOT1* disrupt ER-mitochondria contact sites interfering with calcium homeostasis and mitochondrial dynamics in Parkinson's disease (DOI: 10.1089/ars.2018.7718)
This paper has been peer-reviewed and accepted for publication, but has yet to undergo copyediting and proof correction. The final published version may differ from this proof.

41. Kumar P, Henikoff S, Ng PC. Predicting the effects of coding non-synonymous variants on protein function using the SIFT algorithm. Nat Protoc [Internet]. 2009;4:1073–81. Available from: http://www.ncbi.nlm.nih.gov/pubmed/19561590

42. Adzhubei I, Jordan DM, Sunyaev SR. Predicting functional effect of human missense mutations using PolyPhen-2. Curr Protoc Hum Genet [Internet]. 2013;Chapter 7:Unit7.20. Available from: http://www.ncbi.nlm.nih.gov/pubmed/23315928

43. Schwarz JM, Rödelsperger C, Schuelke M, Seelow D. MutationTaster evaluates disease-causing potential of sequence alterations. Nat Methods [Internet]. 2010;7:575–6. Available from: http://www.ncbi.nlm.nih.gov/pubmed/20676075

44. Reva B, Antipin Y, Sander C. Predicting the functional impact of protein mutations: application to cancer genomics. Nucleic Acids Res [Internet]. 2011;39:e118. Available from: http://www.ncbi.nlm.nih.gov/pubmed/21727090

45. Shihab HA, Gough J, Mort M, Cooper DN, Day INM, Gaunt TR. Ranking non-synonymous single nucleotide polymorphisms based on disease concepts. Hum Genomics [Internet]. 2014;8:11. Available from: http://www.ncbi.nlm.nih.gov/pubmed/24980617

46. Chun S, Fay JC. Identification of deleterious mutations within three human genomes. Genome Res [Internet]. 2009;19:1553–61. Available from: http://www.ncbi.nlm.nih.gov/pubmed/19602639

47. Dong C, Wei P, Jian X, Gibbs R, Boerwinkle E, Wang K, et al. Comparison and integration of deleteriousness prediction methods for nonsynonymous SNVs in whole exome sequencing studies. Hum Mol Genet [Internet]. 2015;24:2125–37. Available from: http://www.ncbi.nlm.nih.gov/pubmed/25552646

48. Zhang Y. I-TASSER server for protein 3D structure prediction. BMC Bioinformatics [Internet]. 2008;9:40. Available from: http://www.ncbi.nlm.nih.gov/pubmed/18215316

49. Sievers F, Wilm A, Dineen D, Gibson TJ, Karplus K, Li W, et al. Fast, scalable generation of high-quality protein multiple sequence alignments using Clustal Omega. Mol Syst Biol [Internet]. 2011;7:539. Available from: http://www.ncbi.nlm.nih.gov/pubmed/21988835

50. Lek M, Karczewski KJ, Minikel E V, Samocha KE, Banks E, Fennell T, et al. Analysis of protein-coding genetic variation in 60,706 humans. Nature [Internet]. 2016;536:285–91. Available from: http://www.ncbi.nlm.nih.gov/pubmed/27535533

51. Grünewald A, Gegg ME, Taanman J-W, King RH, Kock N, Klein C, et al. Differential effects of PINK1 nonsense and missense mutations on mitochondrial function and morphology. Exp Neurol [Internet]. 2009;219:266–73. Available from: http://www.ncbi.nlm.nih.gov/pubmed/19500570

52. Burbulla LF, Schelling C, Kato H, Rapaport D, Woitalla D, Schiesling C, et al. Dissecting the role of the mitochondrial chaperone mortalin in Parkinson's disease: functional impact of disease-related variants on mitochondrial homeostasis. Hum Mol Genet [Internet]. 2010;19:4437–52. Available from: http://www.ncbi.nlm.nih.gov/pubmed/20817635

53. Krebiehl G, Ruckerbauer S, Burbulla LF, Kieper N, Maurer B, Waak J, et al. Reduced basal autophagy and impaired mitochondrial dynamics due to loss of Parkinson's disease-associated protein DJ-1. PLoS One [Internet]. 2010;5:e9367. Available from: http://www.ncbi.nlm.nih.gov/pubmed/20186336

Antioxidants and Redox Signaling
Mutations in *RHOT1* disrupt ER-mitochondria contact sites interfering with calcium homeostasis and mitochondrial dynamics in Parkinson's disease (DOI: 10.1089/ars.2018.7718)
This paper has been peer-reviewed and accepted for publication, but has yet to undergo copyediting and proof correction. The final published version may differ from this proof.

Antioxidants and Redox Signaling
Mutations in *RHOT1* disrupt ER-mitochondria contact sites interfering with calcium homeostasis and mitochondrial dynamics in Parkinson's disease (DOI: 10.1089/ars.2018.7718)
This paper has been peer-reviewed and accepted for publication, but has yet to undergo copyediting and proof correction. The final published version may differ from this proof.

Figure legends

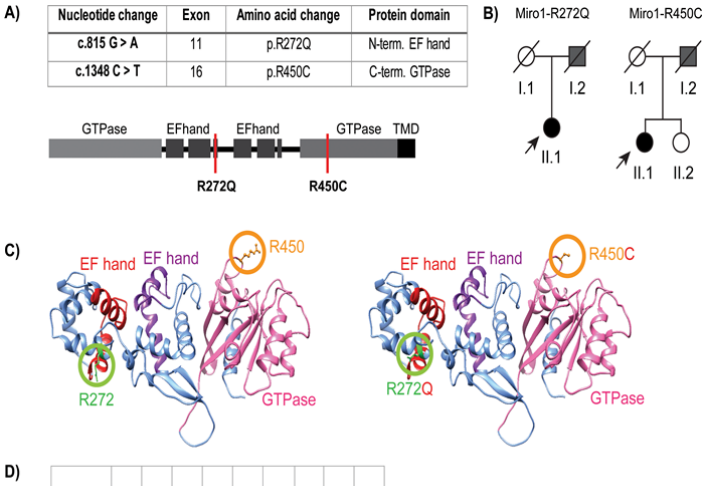

D)

Variant	SIFT	Polyphen2 HDIV	Polyphen2 HVAR	Likelihood ratio test	Mutation taster	Mutation assessor	FATHMM	Radial SVM	LR prediction
R272Q	d	d	d	d	d	h	t	d	d
R450C	d	d	p	d	d	m	t	t	t

E)

Data origin	Sample size	Type of analysis	Variants
Whole Exome Server on neurodegenerative diseases (Tübingen, Germany)	1500 genomes	database	--
662 healthy controls (KORA cohort) 1238 German PD patients	1900 samples	genotyping	--

F)

Constraint from ExAc	Expected no. variants	Observed no. variants	Constraint Metric
Synonymous	124	101	z = 1.62
Missense	362.3	230	z = 2.47
Loss of function	44.9	9	pLI = 0.8
			o/e = 0.2

Figure 1. Identification of R272Q and R450C *RHOT1* variants in PD patients.

A) Table of point mutations identified in *RHOT1* in two PD patients and location of both mutations within the protein structure of Miro1. Miro1 consists of an N-terminal GTPase domain, followed by two EF-hand domains, a C-terminal GTPase domain and a transmembrane domain (TMD). **B)** Pedigree of PD patients with heterozygous point mutations in *RHOT1*. Individuals displaying motor symptoms are highlighted in grey, arrows pointing to PD patients of whom fibroblasts were obtained for the present study. **C)** Left panel: Homology model of wild type human Miro1, covering the 3D protein structure of the both EF-hand domains and the C-terminal GTPase domain. The WT amino acids R272 and R450 are highlighted in circles. Right panel**:** Homology model of mutant

Miro1 with both mutant amino acids R272Q and R450C highlighted in circles. **D)** *In silico* prediction of pathogenic effects of both Miro1 variants. **d**/**h** = deleterious/ highly functional; **p**/**m** = probably damaging/ medium functional; **t** = tolerant. **E)** Genotyping and data mining of a set of PD and control databases to identify additional carriers of the *RHOT1* mutations. The whole exome server on neurodegenerative disease, containing 1500 genomes, was searched for additional carriers of the R272Q and the R450C variants. Additionally, 1900 samples (662 control individuals from the KORA cohort, 1238 German PD patients [14]) were genotyped to confirm our previous findings. No additional carrier of the R272Q or R450C variants were identified. **F)** Burden analysis of variants in *RHOT1* from the gnomAD database. Loss-of-function variants were defined as single nucleotide exchanges causing nonsense, splice acceptor or splice donor variants. **Z-score** = calculated from expected variant counts divided by observed variant counts. **pLI score** = likelihood of a gene to be intolerant to loss-of-function variants. pLI scores close to 1 indicate a high intolerance to loss-of-function variants.

Antioxidants and Redox Signaling
Mutations in *RHOT1* disrupt ER-mitochondria contact sites interfering with calcium homeostasis and mitochondrial dynamics in Parkinson's disease (DOI: 10.1089/ars.2018.7718)
This paper has been peer-reviewed and accepted for publication, but has yet to undergo copyediting and proof correction. The final published version may differ from this proof.

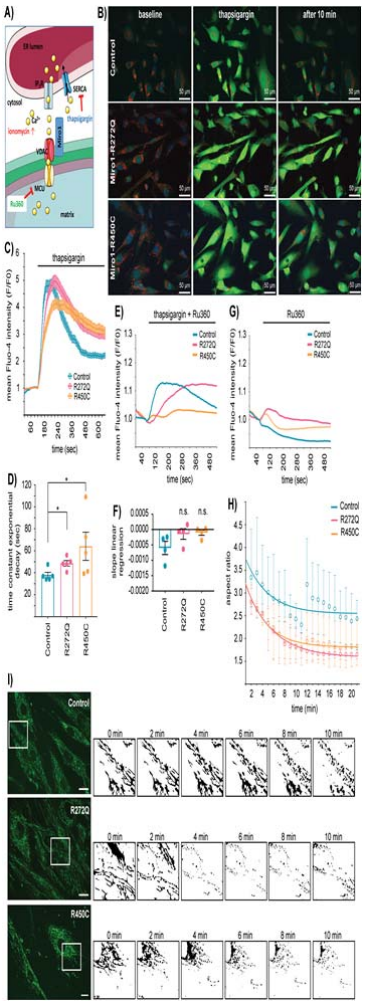

Figure 2. Reduced calcium buffering capacity in Miro1-mutant fibroblasts.

A) Overview of treatments with thapsigargin, ionomycin and Ru360 for calcium imaging. Thapsigargin inhibits calcium uptake of the ER by the SERCA pumps, which leads to increase of cytosolic calcium levels by depletion of ER calcium stores. Ionomycin increases levels of cytosolic calcium by activation of G-protein-coupled receptors in the plasma membrane. Ru360 is an inhibitor of the mitochondrial calcium uniporter (MCU). **B)** Immortalized fibroblasts were loaded with Fluo4-AM (green) for live cell imaging. Cells were imaged under baseline condition for 2 min. After addition of 1 µM thapsigargin, imaging was continued for 10 min with a 2 sec interval. Images were acquired using a 25x objective, scale bars indicate 50 µm. **C)** Quantification of calcium levels upon thapsigargin treatment from B). Mean intensity of Fluo4-AM signal was indicated as (F/F_0). Data indicated as mean ± SEM, n = 5, with 8-20 cells per cell line per experiment. **D)** Time

constant of exponential decay calculated from calcium response curves of C). Data indicated as mean ± SEM. Significance calculated using a Mann-Whitney test (n = 5). **E)** Immortalized fibroblasts were stained with Fluo4-AM for live cell imaging. After 1 min of baseline recording cells were treated with a combination of 10 µM Ru360 and 1 µM thapsigargin, and imaging was continued for 9 min, using a 25x objective (n = 3-4). Data indicated as mean. **F)** Slope of linear regression of calcium response curves from E). Data indicated as mean ± SEM. Significance calculated using a Mann-Whitney test (n = 3-4). **G)** Immortalized fibroblasts were stained with Fluo4-AM and treated with 10 µM Ru360 during live cell imaging. Data indicated as mean (n = 3). **H)** Microscopy images from I) were analysed for aspect ratios of the mitochondrial network over time using ImageJ (n = 3-5). **I)** Immortalized fibroblasts were stained with MitoTracker green FM and treated with 20 µM ionomycin during 20 min of live cell imaging, using a 63x objective. Scale bars indicate 20 µm. Representative images of the mitochondrial network in control fibroblasts, Miro1-R272Q and R450C fibroblasts. Mitochondrial masks generated with ImageJ for the analysis of mitochondrial morphology were displayed at different time points for all cell lines. Significance for all data calculated by Mann-Whitney test. * $p \leq 0.05$ ** $p \leq 0.01$ *** $p \leq 0.001$.

Antioxidants and Redox Signaling
Mutations in *RHOT1* disrupt ER-mitochondria contact sites interfering with calcium homeostasis and mitochondrial dynamics in Parkinson's disease (DOI: 10.1089/ars.2018.7718)
This paper has been peer-reviewed and accepted for publication, but has yet to undergo copyediting and proof correction. The final published version may differ from this proof.

Antioxidants and Redox Signaling
Mutations in *RHOT1* disrupt ER-mitochondria contact sites interfering with calcium homeostasis and mitochondrial dynamics in Parkinson's disease (DOI: 10.1089/ars.2018.7718)
This paper has been peer-reviewed and accepted for publication, but has yet to undergo copyediting and proof correction. The final published version may differ from this proof.

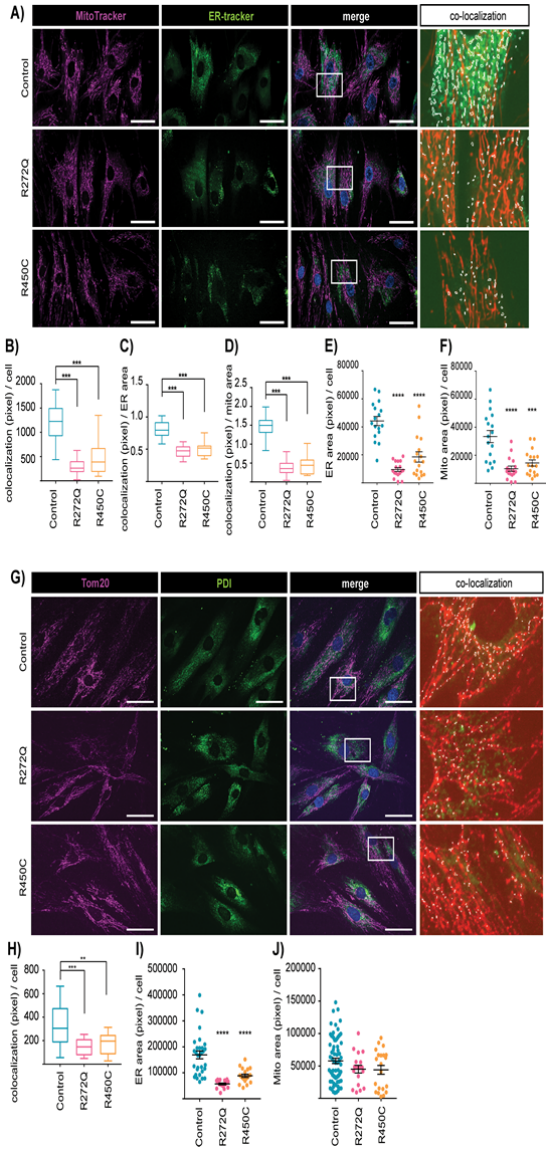

Figure 3. Decreased ER-mitochondrial contact sites in Miro1-mutant fibroblasts.

A) Native fibroblasts were stained with MitoTracker deep red (magenta) and ER-tracker green. Images were obtained with a 40x objective (n = 3). Scale bars indicate 50 µm. Co-localization of ER and mitochondria was analysed in the merged-channel images. The white squares in the merged images indicate the zoomed regions shown for the co-localization panel; co-localization events are highlighted as white dots (see co-localization panel). **B)** Co-localization events of mitochondria and ER pixel from F) were normalized to cell number, **C)** to ER area or **D)** to mitochondrial area. **E)** ER area (pixel) per cell was analysed from live cell microscopy data of ER-tracker. **F)** Mitochondria area (pixel) per cell was analysed from live cell microscopy data of MitoTracker deep red. **G)** Native fibroblasts

were fixed and labelled with antibodies against Tom20 (magenta) and PDI (green) for subsequent immunofluorescent microscopy analysis of mitochondria and ER co-localization. Co-localization of ER and mitochondria was analysed in the merged-channel images. The white squares indicate the zoomed regions shown in the co-localization panel. Co-localization events are highlighted as white dots. Images were obtained with a 40x objective. **H)** Co-localization events of mitochondria and ER pixel from G) were normalized per cell (n = 3, with ~80-90 cells per cell line per experiment). **I)** ER area (pixel) per cell was analysed by quantification of the PDI staining. **J)** Mitochondrial area (pixel) per cell was analysed by quantification of the Tom20 staining. Significance was calculated by Kruskal-Wallis-Test (n = 3). All data indicated as mean ± SEM. * $p \leq 0.05$ ** $p \leq 0.01$ *** $p \leq 0.001$.

Antioxidants and Redox Signaling
Mutations in *RHOT1* disrupt ER-mitochondria contact sites interfering with calcium homeostasis and mitochondrial dynamics in Parkinson's disease (DOI: 10.1089/ars.2018.7718)
This paper has been peer-reviewed and accepted for publication, but has yet to undergo copyediting and proof correction. The final published version may differ from this proof.

Antioxidants and Redox Signaling
Mutations in *RHOT1* disrupt ER-mitochondria contact sites interfering with calcium homeostasis and mitochondrial dynamics in Parkinson's disease (DOI: 10.1089/ars.2018.7718)
This paper has been peer-reviewed and accepted for publication, but has yet to undergo copyediting and proof correction. The final published version may differ from this proof.

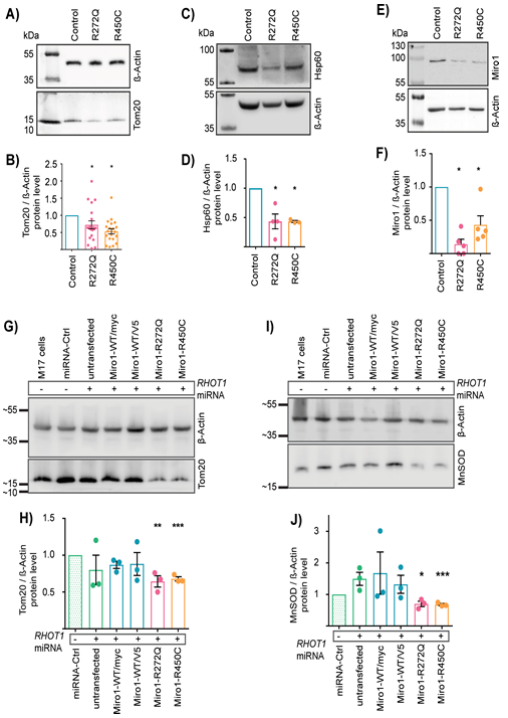

Figure 4. Mutant Miro1 protein leads to reduction of mitochondrial mass.

A) Representative Western blot of Tom20 in immortalized fibroblasts. **B)** Quantification of Tom20 protein level in immortalized fibroblasts from A). Significance tested with a Wilcoxon test (n = 20). **C)** Representative Western blot image of Hsp60 protein in immortalized fibroblasts. **D)** Quantification of Hsp60 normalized to β-Actin from C). Significance assessed using a Mann-Whitney test (n = 4). **E)** Representative Western blot image of Miro1 protein in immortalized fibroblasts. **F)** Quantification of Western blot analysis of Miro1 protein levels from E). Significance determined using a Wilcoxon test (n = 5). **G)** Representative Western blot image of Tom20 and **I)** MnSOD proteins in M17 cells with stable knockdown of endogenous *RHOT1* and transiently overexpression of Miro1 variants. (-) indicates M17 cells without knockdown of endogenous *RHOT1*. (+) indicates knockdown of endogenous *RHOT1* by stable transfection with the *RHOT1*-targeting miRNA-2471 (*RHOT1* miRNA). M17 cells were transfected with Miro1-WT/myc (in pRK5-myc vector), Miro1-WT/V5, Miro1-R272Q or Miro1-R450C (in pcDNA3.1/V5-HisA vector). **H)** Quantification of Tom20 protein levels from G), (n = 3). **J)** Quantification of MnSOD protein levels from I), (n = 3). All data indicated as mean ± SEM. * $p \leq 0.05$ ** $p \leq 0.01$ *** $p \leq 0.001$.

Antioxidants and Redox Signaling
Mutations in *RHOT1* disrupt ER-mitochondria contact sites interfering with calcium homeostasis and mitochondrial dynamics in Parkinson's disease (DOI: 10.1089/ars.2018.7718)
This paper has been peer-reviewed and accepted for publication, but has yet to undergo copyediting and proof correction. The final published version may differ from this proof.

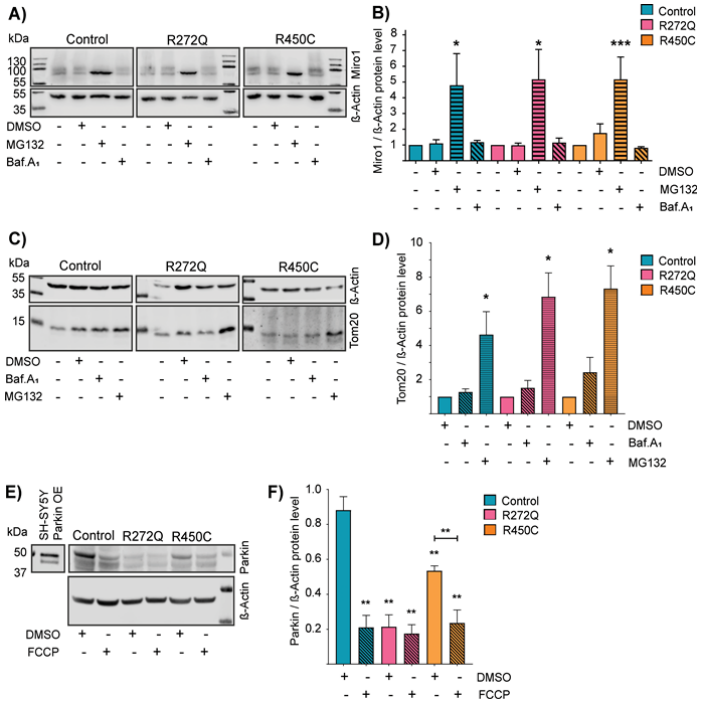

Figure 5. Mitochondrial turnover is increased in Miro1-mutant fibroblasts.

A) Representative Western blot image of Miro1 in immortalized fibroblasts treated with 10 µM MG132 for 24 h or with 10 nM bafilomycinA_1 for 48 h. **B)** Quantification of Miro1 protein level from Western blots displayed in A). Significance assessed with a Wilcoxon test (n = 3-7). **C)** Western blot image for Tom20 protein in immortalized fibroblasts treated with 10 nM bafilomycinA_1 for 48 h or with 10 µM MG132 for 24 h, respectively. **D)** Quantification of Tom20 protein levels from Western blot analysis shown in C). Significance assessed using a Wilcoxon test (n = 5). **E)** Representative Western blot image of Parkin protein. Left panel shows Parkin bands in SH-SY5Y cells overexpressing Parkin. Right panel shows endogenous Parkin in immortalized fibroblasts treated with 10 µM FCCP for 14 hours. **F)** Quantification of Parkin protein levels normalized to β-Actin from E). Significance calculated by Mann-Whitney test (n = 5). All data indicated as mean ± SEM. * $p \leq 0.05$ ** $p \leq 0.01$ *** $p \leq 0.001$.

Antioxidants and Redox Signaling
Mutations in *RHOT1* disrupt ER-mitochondria contact sites interfering with calcium homeostasis and mitochondrial dynamics in Parkinson's disease (DOI: 10.1089/ars.2018.7718)
This paper has been peer-reviewed and accepted for publication, but has yet to undergo copyediting and proof correction. The final published version may differ from this proof.

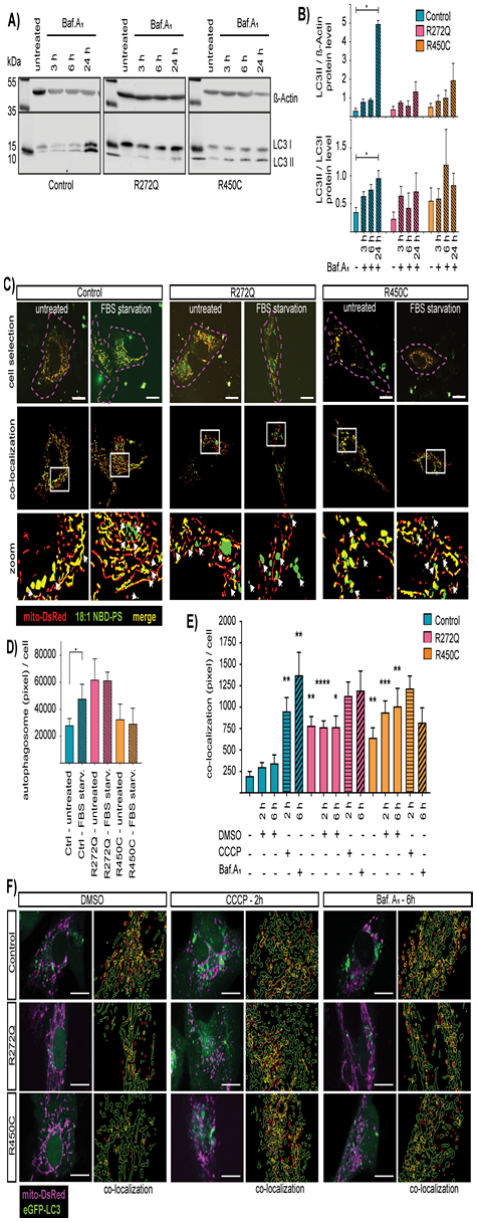

Figure 6. LC3-dependent autophagy is affected in Miro1-mutant fibroblasts.

A) Representative Western blot image of immortalized fibroblasts treated with 10 nM bafilomycinA_1 for 3 hours, 6 hours or 24 hours. **B)** Densitometry analysis of Western blot for LC3-II normalized to β-Actin (upper graph) and the ratio of LC3-II/LC3-I protein levels (lower graph) from A). Significance calculated by Friedman test (n = 3). **C)** Immortalized fibroblasts were transfected with mito-DsRed and labelled with 18:1 NBD PS. Then, cells were starved in medium without FBS for 2 h for subsequent live cell imaging, using a 63x objective. Cell selection shows microscopy images with mito-DsRed-labeled mitochondria

(red) and 18:1 NBD-PS (green). Cells were manually selected (dashed pink outline) in order to ensure that only 18:1 NBD-PS-labeled autophagosomes in the cytosols were analysed. The co-localization panel shows the selected cells from the data analysis. White squares indicate the regions, which were shown in the zoom panel. Autophagosomes were identified as green particles, which are not co-localizing with the mito-DsRed signal (white arrows). **D)** Quantification of autophagosome formation from images shown in C). Significance calculated by Wilcoxon test (n = 3). **E)** Co-localization of mitochondria and LC3 pixel from F) were quantified and normalized to cell number. Significance assessed using a Mann-Whitney Test (n = 3, with ~30 cells per cell line). **F)** Immortalized fibroblasts were transfected with mito-DsRed and eGFP-LC3. 24 h after transfection, cells were treated with 25 µM CCCP or with 10 nM bafilomycinA_1 for 2 h or 6 h, respectively. The left panels show the microscopy images obtained with a 40x objective. The right panels show the co-localization analysis. The outlines of analysed mitochondria are indicated in green, while outlines of analysed LC3 puncta are indicated in red. The co-localization regions of both organelles are indicated in yellow. Scale bars indicate 20 µm. All data indicated as mean ± SEM. * $p \leq 0.05$ ** $p \leq 0.01$ *** $p \leq 0.001$.

Antioxidants and Redox Signaling
Mutations in *RHOT1* disrupt ER-mitochondria contact sites interfering with calcium homeostasis and mitochondrial dynamics in Parkinson's disease (DOI: 10.1089/ars.2018.7718)
This paper has been peer-reviewed and accepted for publication, but has yet to undergo copyediting and proof correction. The final published version may differ from this proof.

Antioxidants and Redox Signaling
Mutations in *RHOT1* disrupt ER-mitochondria contact sites interfering with calcium homeostasis and mitochondrial dynamics in Parkinson's disease (DOI: 10.1089/ars.2018.7718)
This paper has been peer-reviewed and accepted for publication, but has yet to undergo copyediting and proof correction. The final published version may differ from this proof.

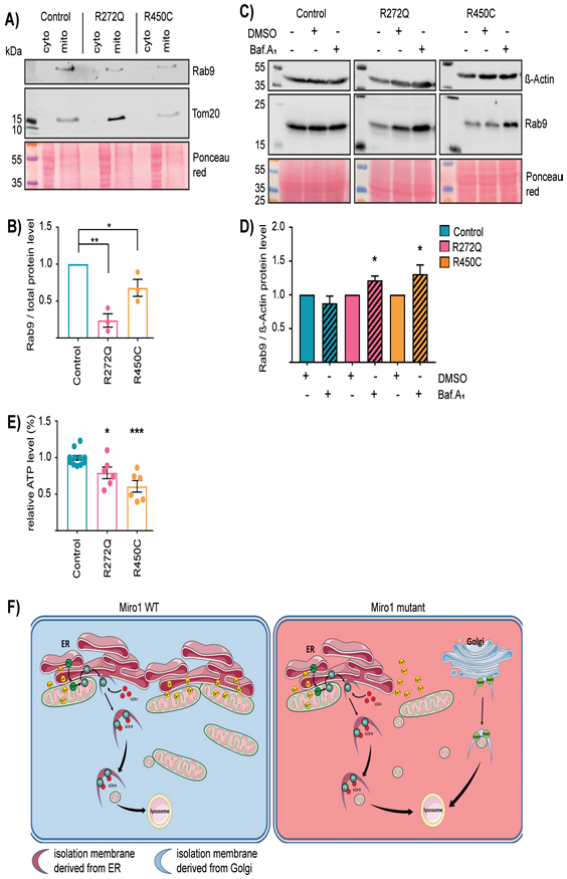

Figure 7. Mutations in Miro1 lead to increased LC3-independent autophagy and impaired energy metabolism.

A) Crude mitochondrial fractions were obtained from immortalized fibroblasts. Rab9 levels were analysed by Western blot. **B)** Quantification of Rab9 protein levels in mitochondrial fractions from A) (n = 3). **C)** Representative Western blot image of Rab9 in whole cell lysates of immortalized fibroblasts treated with 10 nM bafilomycinA_1 for 4 h. **D)** Quantification of Rab9 protein levels from C). Significance determined using a Wilcoxon test (n = 6-11). **E)** Measurement of steady state ATP level under baseline conditions in immortalized fibroblasts. Significance assessed with a Mann-Whitney test (n = 6). **F)** Schematic overview of the mechanism of impaired ER-mitochondria contact sites and increased mitophagy in Miro1 mutant background.

Antioxidants and Redox Signaling
Mutations in *RHOT1* disrupt ER-mitochondria contact sites interfering with calcium homeostasis and mitochondrial dynamics in Parkinson's disease (DOI: 10.1089/ars.2018.7718)
This paper has been peer-reviewed and accepted for publication, but has yet to undergo copyediting and proof correction. The final published version may differ from this proof.

Supplement 1
List of primers targeting exons of *RHOT1* for mutation screen in PD patients

Exon	Exon length (bp)	PCR product (bp)	primer forward (5' > 3')	primer reverse (5' > 3')	Tm
2	59	212	TTG CCA AAT TTG AGC TTA TG	ACA CAT GCC AAA AGA GAC AG	56°C
3	82	230	TTG AGT GAT AAT ATT CAA AGG TGT TT	CCT CTC TGA ACA TTT GTA AAA GC	54°C
4	44	117	CAA TAT GAA ACA TTG ACT TCC TGT C	TTC TAC ACA AAA CCC CAC ACC	61°C
5	54	163	TTG CTA ATT AAG TGC TGT CTA TG	CCA CTG AAA CCA ACT ATA GGG	59°C
6	53	187	GGC TAA GCG CTT GTT AAT TTT C	AAA TTT AAG TGA AGG ATT TAG GGA AG	57°C
7	109	168	CCT TAT TAC AAT GTG CCC TG	AAA TTT TCA AAT CAA ATT ACA AGG	59°C
8	102	378	CAT GTT GTG ATG TCC ACA AAG	ACC AAA ATG TAA CCA TTT AAT AAG C	60°C
9	99	185	CAT TGC TTA TGA AAA TCA CAG	ACG CAA ATG TCT GAA ATA AAG	54°C
10	109	235	GTG GTT TTA ACG CTG GTT TG	CAA TAA AGA CCT TCA CCT TCT GC	57°C
11	121	289	TGC TTT TCT CCT ATG TGA CTC TG	GGT GGG AGG ATC ACT TGA CT	62°C
12	85	209	TGG TGT TAC CTC ACA AAA GAC	TGG AAA ATT ACA GCT AAA GGC	56°C
13	146	2016	TCT AAA CAT TCT GTA TCC TTG TG	TTG TAA CTC TAG AGG AAA GAG GTG	61°C
14	101	198	CCC CAT AAA TAT TCG TTT AGG	AAA TAT CTC TAA TCA TGA GCT GAA C	57°C
15	131	280	GGT GGA ATG GAG GCT TAG TG	CAA TGG CTA TGA AAA CAT TAT GTA AAC	61°C
16	84	195	GCA GAT ATT GAG ATT TTC GGT TC	GAA GCC AAT TTG TTT TCA AAG AG	59°C
17	120	253	TTT TAA ACT TAG GAA GTC CAG GG	CAT TCA GTC ATA GTC TGT AGG AGC	60°C
18	203	393	CTG GAG GAA ATG CTT GGT TC	GTT GCT GAA CAA TTC CTA TGT G	59°C
19	96	178	TTT TAC CTT TGC TTT AAA ACT CTC	CAA CAA AAT CCC ACA GAA G	56°C
20	123	184	TCA ACT CCT GTC CTT CTG TG	GCC TGG TAC CCA GTA AAT AAA G	52°C
21	118	257	CTG GTA TAG GGT TTT CAT ACT AAT C	ATA ATT CTA GCA GAA CTT AAA GCA TTC	56°C

Supplementary Table 1

List of primers used for the *RHOT1* mutation screen in PD patients. Exon lengths were determined using the Genome browser webpage (https://genome.ucsc.edu/cgi-bin/hgTracks?db=hg19&lastVirtModeType=default&lastVirtModeExtraState=&virtModeType=default&virtMode=0&nonVirtPosition=&position=chr17%3A30469473%2D30552746&hgsid=725100075_KGJ3cA6ASUEwBxgtEWZOdDHUrx2K). **bp** = base pairs. **Tm** = annealing temperature of the primers.

Antioxidants and Redox Signaling
Mutations in *RHOT1* disrupt ER-mitochondria contact sites interfering with calcium homeostasis and mitochondrial dynamics in Parkinson's disease (DOI: 10.1089/ars.2018.7718)
This paper has been peer-reviewed and accepted for publication, but has yet to undergo copyediting and proof correction. The final published version may differ from this proof.

Supplement 1
Characterization of knock-down of endogenous *RHOT1* and over-expression of *RHOT1* in M17 cells

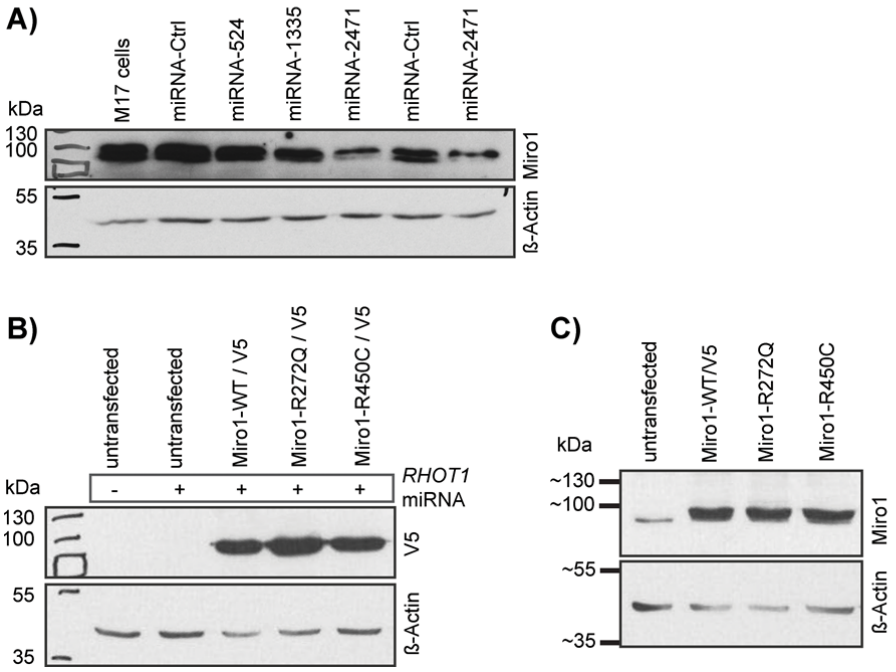

Supplementary Figure 1.

Characterization of knockdown of endogenous *RHOT1* and overexpression of *RHOT1* in M17 cells. **A)** A stable knockdown of endogenous *RHOT1* was established in M17 cells by transfection with miRNAs targeting different regions of *RHOT1* and subsequent selection of positively transfected cells with 6 µg/mL Blasticidin. Knockdown of *RHOT1* was most efficient by using the miRNA-2471, which is targeting the 5'UTR of *RHOT1*. Therefore, we chose the miRNA-2471 for all further experiments. **B)** Representative Western blot image of untransfected M17 cells or M17 expressing different variants of Miro1 in the pcDNA3.1/V5-HisA vector: WT Miro1 (Miro1-WT / V5), Miro1-R272Q and Miro1-R450C. Western blot was probed using an antibody against the V5 tag (Sigma Aldrich, R960-25). Untransfected cells show no signal for V5. **C)** Representative Western blot image of untransfected M17 cells or M17 expressing different variants of Miro1. The Western blot was probed with an antibody against Miro1 (Sigma Aldrich, HPA010687). Untransfected M17 cells show a band for endogenous Miro1, while M17 cells transfected with the pcDNA3.1/V5-HisA vector containing *RHOT1* variants show a strong band for overexpressed Miro1 protein.